Large- and small-scale interactions and quenching in an α^2-dynamo

Peter Frick and Rodion Stepanov
Institute of Continuous Media Mechanics, 1, Korolev, Perm, 614013, Russia

Dmitry Sokoloff
Department of Physics, Moscow State University, 119899, Moscow, Russia

(Received 26 February 2006; revised manuscript received 5 October 2006; published 22 December 2006)

The evolution of the large-scale magnetic field in a turbulent flow of conducting fluid is considered in the framework of a multiscale α^2-dynamo model, which includes the poloidal and the toroidal components for the large-scale magnetic field and a shell model for the small-scale magnetohydrodynamical turbulence. The conjugation of the mean-field description for the large-scale field and the shell formalism for the small-scale turbulence is based on strict conformity to the conservation laws. The model displays a substantial magnetic contribution to the α effect. It was shown that a large-scale magnetic field can be generated by current helicity even solely. The α quenching and the role of the magnetic Prandtl number (P_m) are studied. We have determined the dynamic nature of the saturation mechanism of dynamo action. Any simultaneous cross correlation of α and large-scale magnetic field energy E^B is negligible, whereas coupling between α and E^B becomes substantial for moderate time lags. An unexpected result is the behavior of the large-scale magnetic energy with variation of the magnetic Prandtl number. Diminishing of P_m does not have an inevitable ill effect on the magnetic field generation. The most efficient large-scale dynamo operates under relatively low Prandtl numbers—then the small-scale dynamo is suppressed and the decrease of P_m can lead even to superequipartition of the large-scale magnetic field (i.e., $E_B > E_u$). In contrast, the growth of P_m does not promote the large-scale magnetic field generation. A growing counteraction of the magnetic α effect reduces the level of mean large-scale magnetic energy at the saturated state.

DOI: 10.1103/PhysRevE.74.066310 PACS number(s): 47.27.E−, 52.30.Cv, 95.30.Qd, 91.25.Cw

I. INTRODUCTION

Magnetic fields of celestial bodies are supposed to be generated by a hydromagnetic dynamo operating in a moving electrically conductive medium (see, e.g. [1]). The corresponding flows are characterized by huge values of governing parameters, so a direct numerical simulation (DNS) of the corresponding magnetohydrodynamical (MHD) problem with realistic governing parameters becomes impossible even with modern numerical facilities. Due to rapid progress of numerical facilities the parameter range accessible for DNS is becoming increasingly wide. Some high-resolution simulations of MHD turbulence (up to 1024^3 grid points) have been performed [2,3], which allows one to study the small-scale dynamo processes in detail but does not eliminate the difference of the accessible range from that of the cosmic media (e.g., the magnetic Reynolds number for the interstellar medium is $R_m = 10^6$ even if the estimation of magnetic field losses is based on ambipolar diffusion). Moreover, even if a direct numerical simulation is performed, identification of the large-scale features comparable with observational data is a nontrivial task [4].

The theory of astrophysical dynamos was mainly developed in the framework of the mean-field approach [5]. The mean-field theory is based on the so-called two-scale approximation, which suggests that the magnetic field consists of the large-scale field **B** and the small-scale fluctuations **b**, and that the velocity field is represented as the sum of the mean-field motion **V** and velocity fluctuations **u**. Bearing this in mind some governing equations for large-scale components are evaluated. The transport coefficients in the equations contain some averaged information concerning the small-scale components parametrized in terms of **B** and **V**. This approach yields various models for large-scale magnetic fields of particular celestial bodies, such as galaxies, stars, and planets, which reproduce to some extent the available phenomenology [6]. Various approaches to proper parametrization were suggested (see for review [7,8]). However, the mean-field approach seems to be insufficient because it does not provide an in-depth insight into the evolution of the small-scale magnetic and velocity fields, which are replaced by turbulence parametrization.

It is desirable that the simplicity of the mean-field approach be combined with a relatively simple model of small-scale MHD turbulence, which nevertheless would provide a proper description of interactions of the large-scale magnetic field with the MHD turbulence. This would allow us to avoid the time and resource consuming calculations involved in DNS as well as the insecure parametrizations involved in the mean-field theories.

The shell models were suggested to describe the spectral energy transfer [9,10]. After numerous refinements they became an effective tool for description of the spectral properties of the small-scale turbulence (see for review [11]). These models do not describe the dynamics of turbulent fluctuations **b** and **u** in all details, but replace the full system of governing partial differential equations by some simple ordinary differential equations describing the spectral transfer of energy and other relevant quantities. The shell models for MHD turbulence were introduced in [12–14]. This approach reveals many intrinsic features of the small-scale dynamo action in the fully developed turbulence of conducting fluids [15]. It also allows study of a specific case of a rotating

turbulence [16], which, however, cannot reproduce the dynamics of the mean-field components.

In this paper, we combine the mean-field description of the large scale dynamo with a shell description of the small-scale turbulence over a large range of scales. An attempt to use the shell models for description of the small-scale (subgrid) turbulence has been made in [17] in the context of the problem of convection in a spherical layer. A simple combination of the shell model and the mean-field approach has been suggested in [18] and was developed for the galactic dynamo in [19].

Of particular interest to the mean-field dynamo problems are the mechanisms of dynamo saturation. Conventional mean-field dynamos describe the saturation phenomenon via quenching of dynamo governing parameters, especially α quenching. A simple algebraic quenching implies a direct link between the dynamo governing parameters and the large-scale magnetic field at the same moment in time [20]. Particular forms of algebraic α quenching are considered in [21] (cf. also [22]). More sophisticated formulations are based on magnetic helicity conservation and imply a dynamic link between the alpha effect and the magnetic field [23–26]. An alternative way of quenching description uses the conservation laws. The conservation of magnetic helicity was the basis of quenching in [27–29]. In the framework of our approach we keep all conservation laws and take into account the energy exchange between the large scale field and the turbulent fields to obtain quenching in a self-consistent way.

Another obscure problem of dynamo theory is the role of the magnetic Prandtl number, i.e., the ratio of viscosity ν to magnetic diffusivity ν_m. The MHD dynamo at low magnetic Prandtl numbers has recently become a very hot topic for discussion. The results of DNS for values of the Reynolds number (Re) up to about three orders of magnitude show us that the dynamo threshold is rapidly increased in the laminar range of Re and then the saturated turbulence can stay near $P_m \simeq \text{const}$ [30–32] or the critical value of the magnetic Reynolds number $R_m^* \simeq \text{const}$ [33,34]. These very low values of P_m are available for low-dimensional models of turbulence like the Kasantzev model [35] or shell model. The latter predicts also a saturation of the dynamo threshold [36]. Our approach allowes us to start from the academic case $P_m=1$, and extend our numerical experiments to a very weakly conducting media ($P_m \approx 10^{-8}$).

In this paper we consider the simplest mean-field dynamo problem, namely the so-called "α^2-dynamo." This problem considers the toroidal and poloidal large-scale components of the magnetic field **B** on the assumption that a toroidal field is produced from poloidal by a mechanism similar to that which generates the poloidal component from the toroidal. This mechanism is based on the action of a small-scale helical turbulence and is called the α effect. In reality, the first part of the dynamo cycle (generation of toroidal field from poloidal) is provided by a more effective mechanism—differential rotation (and therefore is called the $\alpha\omega$-dynamo). We use the α^2 problem as an illustrative example of our approach, because the structure of the generated large-scale field is simpler and each component can be described by one mode only [37]. Thus the behavior of the large-scale field can also be considered using the ordinary differential equations. Below, to be specific in the choice of parameters, we shall refer to the local galactic disk dynamo problem.

The structure of the paper is as follows. The α^2-dynamo problem is described in Sec. II. In Sec. III the shell model of MHD turbulence with a controlled injection of helicity is introduced. The main question concerning conjugation of these two approaches is described in Sec. IV. Here bearing in mind the link between the shell model and the large-scale variables, we have based our choice on the conservation laws requiring that our model should correctly reproduce all conservation laws known in MHD. The crucial role of the conservation laws is well known, both in the context of the shell models for pure hydrodynamics and for MHD turbulence. The conservation laws effectively restrict the freedom in constructing the shell models. The remaining freedom allows some divergence between the detailed descriptions of spectral properties of magnetic and velocity fluctuations, but does not affect the basic features of the turbulence evolution. We will demonstrate that these observations are valid for our combined models, at least for the case of α^2 dynamos. In Sec. V we present the numerical results which concern the saturation mechanism, the role of dynamic and magnetic contributions to the α effect, and the dynamo action under a wide range of the magnetic Prandtl number. A general discussion is presented in Sec. VI.

II. α^2-DYNAMO

The simplest large-scale dynamo model defined in terms of poloidal B_P and toroidal B_T components of the magnetic field can be represented by the following dimensionless equations:

$$d_t B_P = ik_L \alpha B_T - k_L^2 \beta B_P, \tag{1}$$

$$d_t B_T = -ik_L \alpha B_P - k_L^2 \beta B_T. \tag{2}$$

The integral scale of turbulence l is used here as the unit of length. $k_L=(l/L)$ is the normalized wave number, where L corresponds to the scale of the whole system (e.g., the computational domain for the large-scale variables). In principle, we could set l equal to L by taking $k_L=1$ and use the first shell as basic scale which is common practice in the theory of turbulence. We prefer to have k_L as an independent parameter bearing in mind that in many astrophysical models of dynamo action l should be substantially lower than L (see for review [6]).

α describes the capacity of helical small-scale turbulence for generation of the mean large-scale magnetic field, and β is the effective diffusivity of the turbulent media. Thus the poloidal field is generated from the toroidal by the alpha effect, just as the toroidal field is generated from the poloidal, and they are both affected by turbulent diffusion. This is just the process known as the α^2-dynamo.

The mean-field concept estimates β from the turbulent energy as $\beta=\tau\langle u^2\rangle/3$ and α from the helicity of turbulence $\chi^\mu=\langle \mathbf{u}\cdot(\boldsymbol{\nabla}\times\mathbf{u})\rangle$ as $\alpha=-\tau\chi^\mu/3$, where τ is a "memory time." The question arises as to what quantity can be chosen for τ.

A simple estimation for τ is the turnover time for the basic scale of turbulence or its correlation time. The naive estimation here is the relation $\tau=l/u$, where u is r.m.s. velocity. Such a parametrization in the spirit of the mixing length theory is sufficient for many astrophysical models, but it ignores the spectral properties of the turbulence while our intention is to take them into consideration.

A more advanced parametrization of the turbulent transport coefficients β and α follows from the Kolmogorov description of turbulence as an ensemble of vortices of various scales. Then β and α are determined by contribution from the whole spectral range as

$$\beta = \frac{1}{3}\int \tau(k)E(k)dk, \tag{3}$$

$$\alpha = \frac{1}{3}\int \tau(k)\chi^{u}(k)dk. \tag{4}$$

Here $E(k)$ is the energy spectral density and $\chi^{u}(k)$ is the helicity spectral density, $\chi^{u}=\int\chi^{u}(k)dk$. The natural estimate for $\tau(k)$ is the turnover time of the vortex of the corresponding scale or the time averaged with the energy weight. For Kolmogorov's turbulence $E(k)\sim k^{-5/3}$, $\tau(k)=k^{-2/3}$ and according to Eq. (3) β is determined by the integral scale of the turbulence. Note that β is determined by the integral (macro) scale even if we choose $\tau(k)=$const. The situation with α is more delicate. The upper bound for $\chi^{u}(k)$ for Kolmogorov's turbulence is $k^{-2/3}$. If one uses $\tau(k)=$const in Eq. (4) then α is determined by the microscale of the turbulence. A more adequate choice $\tau\sim k^{-2/3}$ means that α as well as β are determined by a macroscale.

Equations (1) and (2) result in the exponential growth of the magnetic field provided the induction effects described by terms with αk_L are large compared to the losses βk_L^2. Saturation of the exponential growth is however impossible for the given α and β, and some modification of their values is required. The simplest argument is that the Lorentz force suppresses the helicity and modifies α. This kind of dynamo saturation is known as α quenching.

An alternative understanding of dynamo saturation is based on the idea of a possible counteraction of the small-scale magnetic field to the turbulent dynamo and can be presented as follows. The dynamo generated magnetic field appears to be mirror asymmetric as well as the velocity field. The degree of magnetic mirror asymmetry can be described, e.g., by the so-called current helicity $\chi^{j}=\langle\mathbf{b}\cdot\mathbf{j}\rangle$. A magnetic contribution α^{b} to the α effect was suggested initially in [38] as

$$\alpha = \alpha^{u} + \alpha^{b}. \tag{5}$$

This way of dynamo saturation was recently developed in some papers (see, e.g., [21,23,27–29]). The physical meaning of this equation can be presented as follows. α effect is associated with mirror symmetry breaking in the system. If a magnetic field is weak the symmetry breaking is related with the velocity field only (it gives α^{u}). A substantial magnetic field can also disturb the mirror symmetry and contribute to α, which gives α^{b}. This concept was supported by calculation of the turbulent electromotive force in various models (see, e.g. [24] and references therein).

III. SHELL MODEL OF MHD TURBULENCE

Shell models are designed to describe the cascade process over a large range of scales (wave numbers) by a chain of variables $u_n(t)$, $b_n(t)$, each of them characterizing all velocity or magnetic field oscillations with wave numbers k in the range from $k_n=k_0\lambda^n$ to k_{n+1} (i.e., a shell of wave numbers). The parameter λ characterizes the ratio of two adjacent scales (the width of the shell) and usually $\lambda\leqslant 2$. The model includes a corresponding set of ordinary differential equations, which should reproduce the basic properties of the motion equation. Namely, the model has to reproduce the type of nonlinearity of the initial equations and to retain the same integrals of motion in the dissipationless limit. Let us note that shell models can possess positively defined integrals of motion [energy, enstrophy in two-dimensional (2D) turbulence, and the square of magnetic potential in 2D MHD turbulence], as well as quadratic integrals with an arbitrary sign (the integrals of this kind are usually called "helicities"). The signs of the helicities are defined by the balance between the contributions of odd and even shells to corresponding quantity.

Let us explore the shell model of MHD turbulence, introduced in [14]. The ordinary differential equations for the shell variables are written as

$$\left(d_t + \frac{k_n^2}{\mathrm{Re}}\right)u_n = ik_n\left\{u_{n+1}^{*}u_{n+2}^{*} - b_{n+1}^{*}b_{n+2}^{*} + \frac{1-\lambda}{\lambda^2}(u_{n-1}^{*}u_{n+1}^{*} - b_{n-1}^{*}b_{n+1}^{*}) - \frac{1}{\lambda^3}(u_{n-2}^{*}u_{n-1}^{*} - b_{n-2}^{*}b_{n-1}^{*})\right\} + F_n, \tag{6}$$

$$\left(d_t + \frac{k_n^2}{\mathrm{R_m}}\right)b_n = \frac{ik_n}{\lambda(1+\lambda)}\{(u_{n+1}^{*}b_{n+2}^{*} - b_{n+1}^{*}u_{n+2}^{*}) + (u_{n-1}^{*}b_{n+1}^{*} - b_{n-1}^{*}u_{n+1}^{*}) + (u_{n-2}^{*}b_{n-1}^{*} - b_{n-2}^{*}u_{n-1}^{*})\} + G_n. \tag{7}$$

These equations are represented in dimensionless form, $\mathrm{Re}=Ul/\nu$, where Re is the Reynolds number, $R_m=Ul/\nu_m$ is the magnetic Reynolds number, d_t is the time derivative, U is the characteristic velocity at the turbulent integral scale, F_n describes forces, and G_n describes currents, acting on the corresponding scales (in the following, for the sake of brevity, we will call them "forces"). The time unit is defined as the turnover time of the vortex on the largest turbulent scale. Equations (6) and (7) take into account the local nonlinear interactions only. In the dissipationless force-free limit ($F_n=G_n=0$, Re, $R_m\to\infty$) they conserve three quadratic quantities, which correspond to the three integrals of motion known in 3D magnetohydrodynamics: The total energy $E=E^{u}+E^{b}$ (where $E^{u}=\Sigma|u_n|^2$ and $E^{b}=\Sigma|b_n|^2$), the cross helicity $\chi^{c}=\Sigma(u_nb_n^{*}+b_nu_n^{*})$, and the magnetic helicity $\chi^{b}=\Sigma(-1)^n|b_n|^2/k_n)$. Note that in the kinematic limit (all $b_n\to 0$) Eq. (6) also conserves the quantity $\chi^{u}=\Sigma(-1)^nk_n|u_n|^2$, which

corresponds to the hydrodynamic helicity, which is the second integral of motion in 3D hydrodynamics. The shell model has some proxy of helicity (the topological meaning of helicity is lost). However, we suppose that this "helicity-like" integral of motion is related to α and, as will be shown below, it works well in the sense that the model reproduces the expected properties of α^2-dynamo.

The forces F_n and G_n include several terms

$$F_n = f_n^I + f_n^C + f_n^B, \tag{8}$$

$$G_n = g_n^I + g_n^B. \tag{9}$$

The terms f_n^I and g_n^I describe the external energy sources. Because we are interested in the dynamo problem we assume that $g_n^I \equiv 0$. The force f_n^I injects kinetic energy and maintains the turbulent flow. We consider f_n^I, acting in the two largest neighboring shells $n=0$ and $n=1$, as a complex value with constant module and phase changing randomly after each t_c unit of time (t_c can be considered as a correlation time).

In the case of pure hydrodynamics this force is usually taken in a simpler form $f_0^I = c(1+i)$, which provides a chaotic solution with a stable spectral energy flux and robust statistical characteristics [15,39]. The MHD system under the same forcing and weak initial magnetic energy describes the small-scale dynamo processes leading to a developed MHD turbulence, with equipartition of the magnetic and kinetic energy and spectral index close to "−5/3" [14]. This state seemed to be statistically stable, but long-time simulations have shown that after relatively long evolution (hundreds of turnover times) this state is often replaced by another one, characterized by a high level of cross correlations ($\langle u_n b_n \rangle \sim \langle u_n^2 \rangle \sim \langle b_n^2 \rangle$), steep spectra, and blocked spectral flux [40,41]. The force with a randomized phase allows us to avoid these highly correlated states.

The terms f_n^B and g_n^B describe the reaction of the large scale magnetic field onto small scale variables. They will be defined in the next section.

Figure 1 shows a typical time evolution of hydrodynamic helicity χ^u and normalized cross helicity $\chi_*^c = \chi^c / (E^u E^b)^{1/2}$ (which characterizes the level of u_n and b_n correlation), and the spectra, obtained from numerical simulations of Eqs. (6) and (7) for $\mathrm{Re} = R_m = 10^6$. Note that both characteristics display intensive irregular oscillations, while their mean value is rather close to zero. The mean value χ_*^c is about −0.1 which directly indicates an uncorrelated behavior of the magnetic and kinetic variables. For the given time interval the mean value of helicity was $\langle \chi^u \rangle = -0.4$ and shows that the model displays a weak helical (on the average) behavior. For longer averaging times this value becomes lower (see Fig. 2), but remains stably negative. This asymmetry reflects a generic shortcoming of the shell models: The discrete nature of these models violates the balance of the odd and even shells when the spectrum decreases with k.

It is commonly believed that the fully developed turbulence is mirror symmetric, namely nonhelical, unless some external sources of mirror asymmetry exist. In astrophysical applications of the mean-field dynamo models one expects the occurrence of helical turbulence, the source of which is

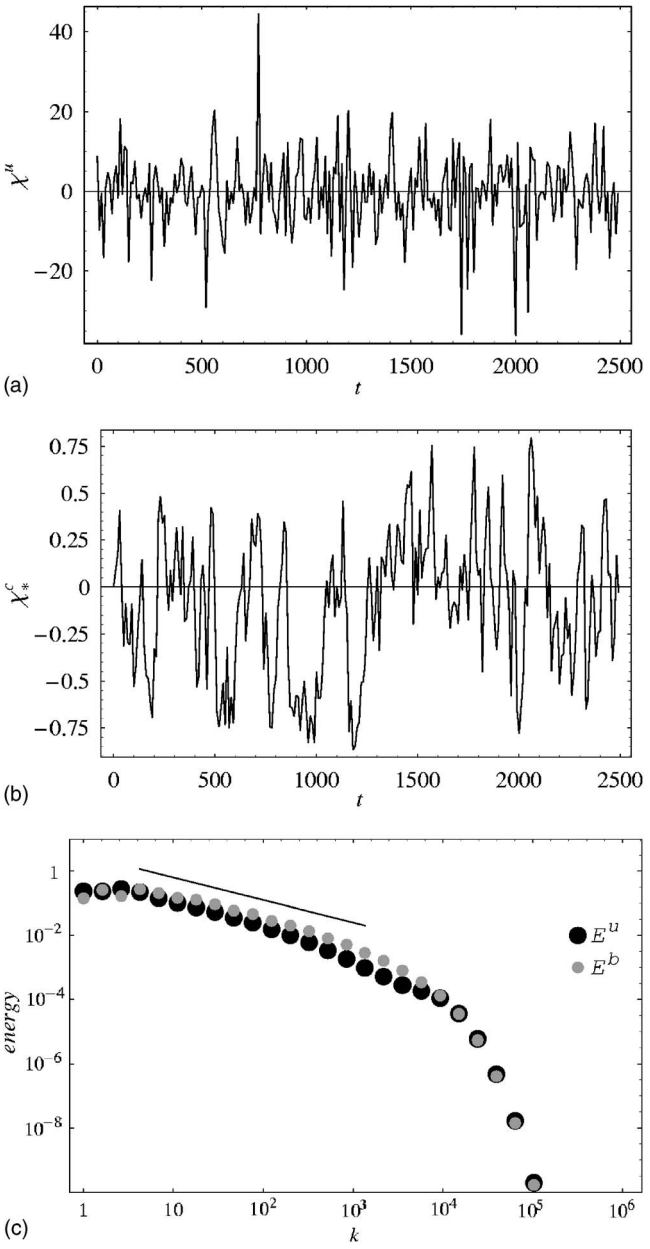

FIG. 1. Simulations of the shell model of forced MHD turbulence. Evolution of (a) hydrodynamic helicity χ^u and (b) normalized cross helicity χ_*^c. The energy spectra (c) for the velocity field E^u (black dots) and the magnetic field E^b (gray dots). The solid line shows the Kolmogorov spectrum slope.

thought to be related to the rotation of celestial bodies. In the framework of shell models conformable to the definition of helicities, "helical" means the asymmetry of even and odd shells. In the model under discussion a source of helicity is necessary, which is directly controlled by some parameter. To this end we introduce a force

$$f_n^C = C(-1)^n \frac{|u_n|^2 + |u_{n+1}|^2}{|u_n|^2} u_n, \tag{10}$$

which redistributes the energy of odd and even shells without any input or output of total energy. The parameter C specifies

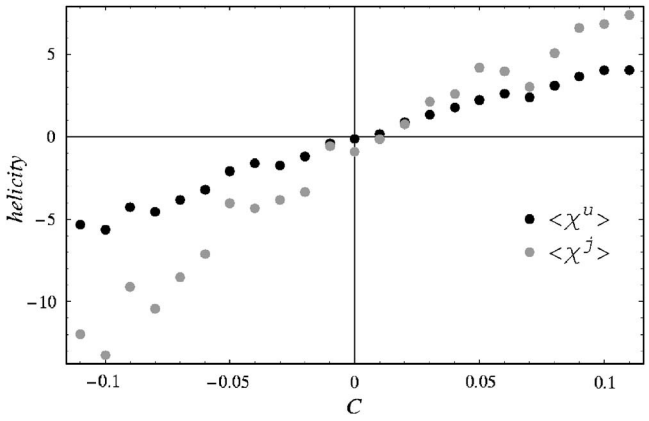

FIG. 2. Mean hydrodynamic helicity $\langle \chi^u \rangle$ (black) and mean current helicity $\langle \chi^j \rangle$ (gray) versus the parameter C defining the mirror asymmetry of the shell model. No mean magnetic field is present.

the degree of mirror asymmetry, defining the part of redistributed energy. Figure 2 shows that $\langle \chi^u \rangle \sim C$ in a wide range of C. The large value of C ($|C| > 0.1$) destroys the turbulent cascade and the small-scale motions occur at a considerable distance from the Kolmogorov turbulence. Note, however, that the turbulence in rapidly rotating bodies, like the Earth, is also far from Kolmogorov. The mean value of the current helicity $\langle \chi^j \rangle$, which provides the magnetic contribution to the alpha effect, is also shown in Fig. 2. Although the force f^C does not directly affect the variables B_n, the level of $\langle \chi^j \rangle$ is mainly higher than $\langle \chi^u \rangle$.

Let us note that the model under consideration produces a large-scale magnetic field with vanishing magnetic helicity in a thin disk. It means that the main effect leading to magnetic contribution to the α effect, i.e., sharing (redistribution) of magnetic helicity between the large-scale and small-scale magnetic variables, does not work in the model (recall that it is just the magnetic helicity that is conserved by the MHD equations). According to naive expectation, we should not obtain any significant magnetic contribution to the α effect. Because the dynamics of the magnetic and current helicity is rather complicated, the analytical papers traditionally ignore the possibility of creating the magnetic α effect for large-scale magnetic fields with vanishing magnetic helicity (cf. however [42]).

IV. COMBINED MODEL

The model is based on the combination of large-scale equations (1) and (2) and shell equations (6) and (7). The coefficients α are calculated from the shell model as well as the turbulent diffusivity β:

$$\alpha^u = -\frac{1}{3}\sum_n \tau_n \chi_n^u = -\frac{1}{3}\sum_n (-1)^n \tau_n k_n |u_n|^2, \tag{11}$$

$$\alpha^b = \frac{1}{3}\sum_n \tau_n \chi_n^j = \frac{1}{3}\sum_n (-1)^n \tau_n k_n |b_n|^2, \tag{12}$$

$$\beta = \frac{1}{3}\sum_n \tau_n |u_n|^2 + \eta, \tag{13}$$

where η describes the ohmic dissipation (in nondimensional units $\eta = R_m^{-1}$) and the correlation time τ_n for a given scale n is taken from Kolmogorov's estimate.

The terms F_n and G_n in shell equations (6) and (7) should be specified taking into account the energy exchange between the large and small scales. It is important to allow for the energy, which is used by turbulence to generate the large-scale magnetic field. It is evident that this energy must be removed from the turbulence by the appropriate correction of variables u_n. This correction is provided by terms f_n^B and g_n^B.

We proceed from the simplest reasoning that each shell must lose as much energy as it produces in the large scale magnetic field due to the α effect. Part of the large-scale energy $E^B = |B_T|^2 + |B_P|^2$ generated by the α effect is

$$E_n^{\alpha^u} = 2ik_L \alpha_n^u (B_T B_P^* - B_P B_T^*), \tag{14}$$

$$E_n^{\alpha^b} = 2ik_L \alpha_n^b (B_T B_P^* - B_P B_T^*). \tag{15}$$

On the other hand, the large-scale magnetic field loses energy due to turbulent diffusivity (the β effect). The turbulent velocity field transfers this energy

$$E_n^\beta = k_L^2 \beta_n E^B \tag{16}$$

to the energy of small-scale magnetic fluctuations. This exchange should also obey the second conservation law concerning the magnetic helicity. Because the large scale magnetic field is nonhelical according to the governing equations of the α^2-dynamo, this conservation law requires that the forces f_n^B and g_n^B should not induce magnetic helicity in the small-scale magnetic field. The third condition is provided by the total cross helicity conservation law. Then the forces f_n^B and g_n^B are defined as

$$f_n^B = -\frac{E_n^{\alpha^u} B_n}{U_n^* B_n - U_n B_n^*}, \tag{17}$$

$$g_n^B = -\frac{U_n Q_n}{B_n^* U_n - B_n U_n^*}, \tag{18}$$

$$Q_n = \begin{cases} \dfrac{(E_n^{\alpha^b} + E_{n+1}^{\alpha^b} - E_n^\beta - E_{n+1}^\beta)}{\lambda + 1}, & n \text{ even}, \\ \dfrac{(E_n^{\alpha^b} + E_{n-1}^{\alpha^b} - E_n^\beta - E_{n-1}^\beta)\lambda}{\lambda + 1}, & n \text{ odd}. \end{cases} \tag{19}$$

Thus our combined model consists of Eqs. (1) and (2) for the large-scale magnetic field and Eqs. (6) and (7) including the forces (8) and (9) for the small-scale turbulence. It should be noted that this system in the limit $f_n^I \to 0$ (no energy input) and $\mathrm{Re}, R_m \to \infty$ (no dissipation) conserves the total energy $E = E^B + E^u + E^b$.

Based on the proposed model we carried out numerical simulation using the fourth order Runge-Kutta method with a fixed time step $\tau = 5 \times 10^{-5}$ for the following set of parameters: $\lambda = (\sqrt{5}+1)/2$, $n = 1, \ldots, 30$, $\mathrm{Re} = R_m = 10^6$, and the cor-

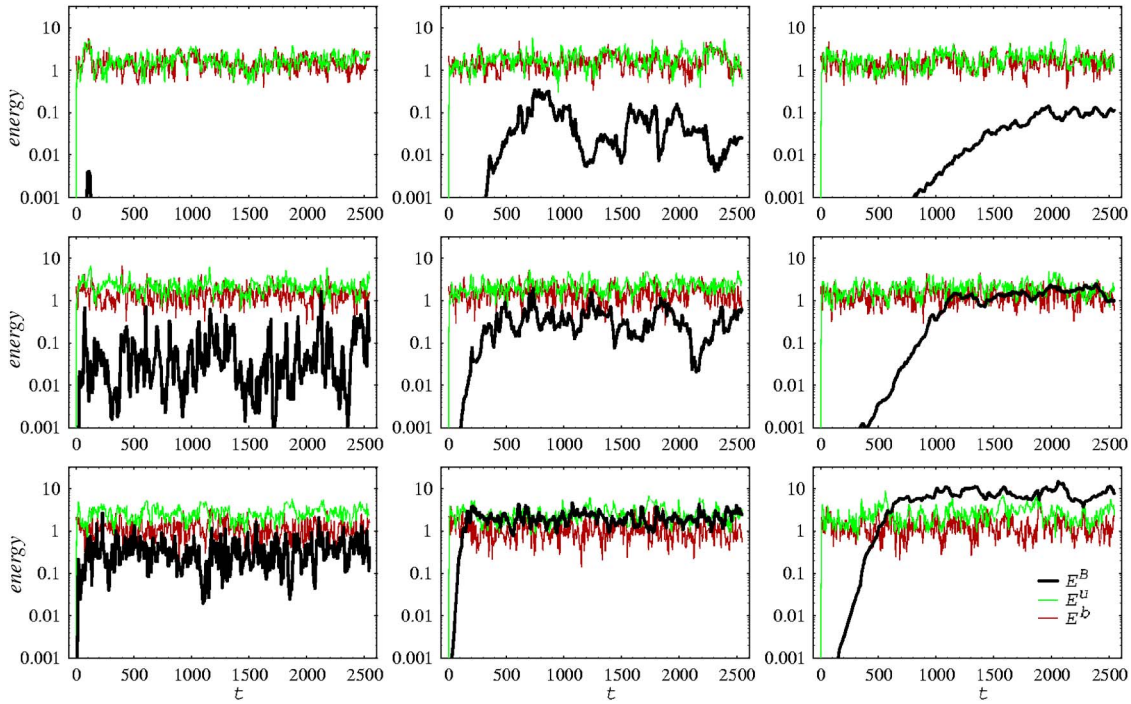

FIG. 3. (Color online) Time series for the mean magnetic field energy E^B (thick black line), small-scale magnetic energy E^b (thin light line, or green line in color version), and kinetic energy E^u (thin dark line, or red line in color version). The horizontal rows correspond to $C=0$, 0.04, and 0.16 (from top to bottom). Vertical columns correspond to $k_L=1/2$, $1/8$, and $1/32$ (from left to right). The magnetic field does not contribute to the α effect ($\alpha^b=0$).

relation time for the force $\tau_c=0.01$. All simulations were performed for the following set of governing parameters: $C=0, \pm 0.01, \pm 0.02, \pm 0.04, \pm 0.08, \pm 016, \pm 0.32$ and $k_L=1/2, 1/4, 1/8, 1/16, 1/32$. In figures given below only a small (but instructive) part of the time series obtained is shown.

V. RESULTS

First, we include in our consideration all saturation mechanisms except the magnetic contribution to the α effect. The reason is that, in dynamo theory, the physics and parametrization of the magnetic α effect is far from completely understood. It looks reasonable to separate the role of the magnetic contribution to the α effect from the other contributions as far as possible. Shown in Fig. 3 are some typical time series for the kinetic E^u and magnetic E^b energy of the turbulent (small-scale) fluctuations and of the large-scale magnetic energy E^B evolution. The results are given for increasing contribution of the force f_n^C and for three values of k_L.

The general result is that the small-scale magnetic energy rapidly, i.e., in several turnover times, achieves equipartition with the kinetic energy while the evolution of the large-scale field is much slower and depends on the intensity of the mirror asymmetry of the small-scale variables and on the scale k_L.

As might be expected from the kinematic dynamo theory, the magnetic field decays at weak α effect and grows when it is strong. The critical value of α, which defines the threshold of the large-scale magnetic field self-excitation, becomes lower for smaller values of k_L. The reason is that the generation of the large-scale magnetic field due to the α effect is proportional to k_L while the dissipation due to turbulent diffusion is proportional to k_L^2.

Note that $C=0$ gives a nonvanishing $\langle\alpha\rangle$, which suggests that a large-scale magnetic field can be excited. It was found that α^u is no longer symmetric with respect to C in the presence of large-scale magnetic field, even when this field is weak. In this sense, a weak large-scale magnetic field affects the mean-field dynamo substantially. We found that the value $C=-0.03$ provides $\langle\alpha\rangle\approx 0$, so the dynamo action is approximately symmetric with respect to $C=-0.03$.

In contrast to the kinematic models, the excitation threshold in the model is not abrupt. For a substantial parameter range the large-scale magnetic field demonstrates a marginal behavior where epochs of temporal growth and epochs of temporal decay occur intermittently. A reverse reaction of the growing magnetic field onto the generation becomes substantial for a rather low large-scale magnetic field strength. However, the growing large-scale magnetic field usually reaches a level comparable to the equipartition level.

A decrease of k_L results in a more effective generation for any C, but essentially increases the time scale of the large-scale energy evolution. The time series become more and more smooth as might be expected under the two-scale approach.

If k_L becomes large (comparable with unity) the time scale for the large-scale magnetic field decreases and becomes comparable with the time scales typical for turbulence on the integral scale. Then the mean-field dynamo concept

becomes inadequate. A smooth behavior of the large-scale variables expected under the mean-field approach is achieved provided that k_L becomes small enough. In practice, the value $k_L \approx 0.3$ seems to be an upper limit for applicability of the mean-field concept. Note that the galactic turbulence has k_L compatible with this requirement ($l \approx 100$ pc and thickness of the galactic disk $L \approx 1$ kpc).

If C increases, the corresponding increase of kinetic helicity intensifies the generation process. For high C and low k_L the energy of the large-scale magnetic field becomes even larger than the kinetic energy of the turbulence responsible for its generation (see the right hand panel in the lower row of Fig. 3). This state is often referred to as superequipartition.

A. Nonlinear hydrodynamic stabilization of dynamo

From Fig. 3 we conclude that the large-scale generation somehow arrives at a saturated state for any value of the governing parameters C and k_L. One of the supposed mechanisms of dynamo saturation implies direct suppression of the α effect by the large-scale magnetic field (the so-called α quenching). Our aim now is to test this concept in the frame of our model. Recall that up to now we have excluded the term α^b from consideration.

Before proceeding to particular results we will point out several obstacles to this verification. The mean-field theory considers the *mean* value of α whereas in our treatment we deal with the current value, which seems to be consistent with the physical nature of the problem. The saturation appears as a dynamically stabilized state, which we analyze studying the cross correlations of α and the energy of the large-scale magnetic field.

The cross-correlation function for the large scale magnetic energy and α^u is defined as

$$\delta(\tau) = \frac{\int \tilde{E}^B(t)\tilde{\alpha}^u(t+\tau)dt}{\left(\int (\tilde{E}^B)^2(t)dt \int (\tilde{\alpha}^u)^2(t)dt\right)^{1/2}}, \qquad (20)$$

where the tilde means the deviation from the mean value. The cross correlation is calculated using a very long time series (about 20000 turnover time units). Figure 4 shows this function for $C=0.08$ and two values $k_L=1/2$ and $k_L=1/16$. The figure shows that the cross correlation is mainly positive for $\tau>0$ and negative for $\tau<0$. The correlation vanishes when the time lag $|\tau|$ becomes large enough. The large k_l, the narrower the range where the cross correlation exceeds the noise.

For negative τ (then E^B follows α) the negative α^u leads to generation of E^B with a relatively short characteristic time shift (the negative peak appears at $\tau=-2.5$ turnover times for $k_L=1/2$ and at $\tau=-7.5$ turnover times for $k_L=1/16$). For positive τ (α follows E^B) the reverse reaction is much slower and we get a positive maximum for $10<\tau<250$ ($k_L=1/16$). It means that E^B produces positive α which counteracts the dynamo. For $k_L=1/2$ the time of the positive reaction is shorter (up to $t \approx 50$). However, the structures of both cross-correlation functions are similar. Let us recall that by definition the sign of α is opposite to that of the hydrodynamic helicity χ^u [see Eq. (7)], so that a positive C leads to production of a negative mean α.

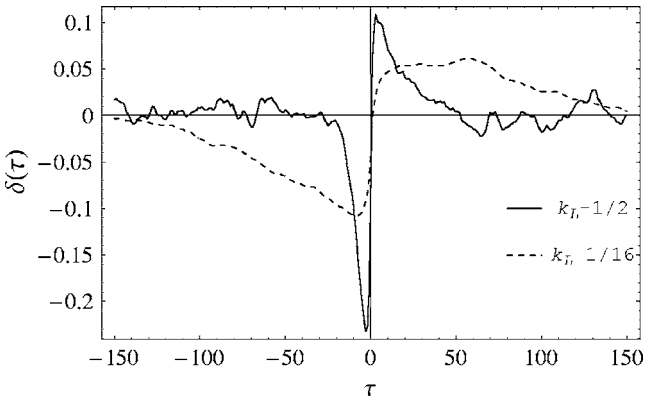

FIG. 4. Cross-correlation function $\delta(\tau)$ of the large scale magnetic field and α^u for $C=0.08$; $k_L=1/2$ (solid) and $k_L=1/16$ (dashed).

From the above follows the conclusion that because the instantaneous correlation of the magnetic field and α vanishes, the naive algebraic quenching is inadequate for the problem. This looks reasonable since the model includes a physical process responsible for quenching while the mean-field theory ignores time scales shorter than those of the large-scale variables. The pronounced (although moderate) lag in the cross correlation means that quenching is described by a differential equation. A reconstruction of this equation from the shape of the cross-correlation function would be an obvious overestimation of the abilities of the model. Though the maximal values of the cross-correlation are rather moderate they prove to be meaningful because we deal with fluctuations around a steady state. A similar time lag between the magnetic field growth and α effect has been observed in DNS of the disk $\alpha\omega$-dynamo [4].

B. The role of the magnetic contribution to the α effect

To determine the contribution of the magnetic field to the alpha effect we have performed simulations taking into account only the magnetic part of the α effect $\alpha=\alpha^b$ ($\alpha^u \equiv 0$). Figure 5 shows the time series of the kinetic E^u and magnetic E^b energy of turbulent (small-scale) pulsations and of the large-scale magnetic energy E^B evolution for the same set of parameters C and k_L as was used in Fig. 3. The general shape of the large-scale magnetic field evolution remains basically the same as for the hydrodynamic alpha effect. For small values of C the generation is even more effective (compare the first rows in both figures). By contrast, at large C (last rows in Figs. 3 and 5) the magnetic alpha effect is less effective for large-scale field generation.

This rather artificial experiment confirms the concept that the dynamo action can occur via magnetic contribution to the α effect only. This point of view was advanced by Vainshtein [43] (see also [44]).

As a next step we performed the same set of simulations for the full model ($\alpha=\alpha^u+\alpha^b$). The corresponding time series are shown in Fig. 6.

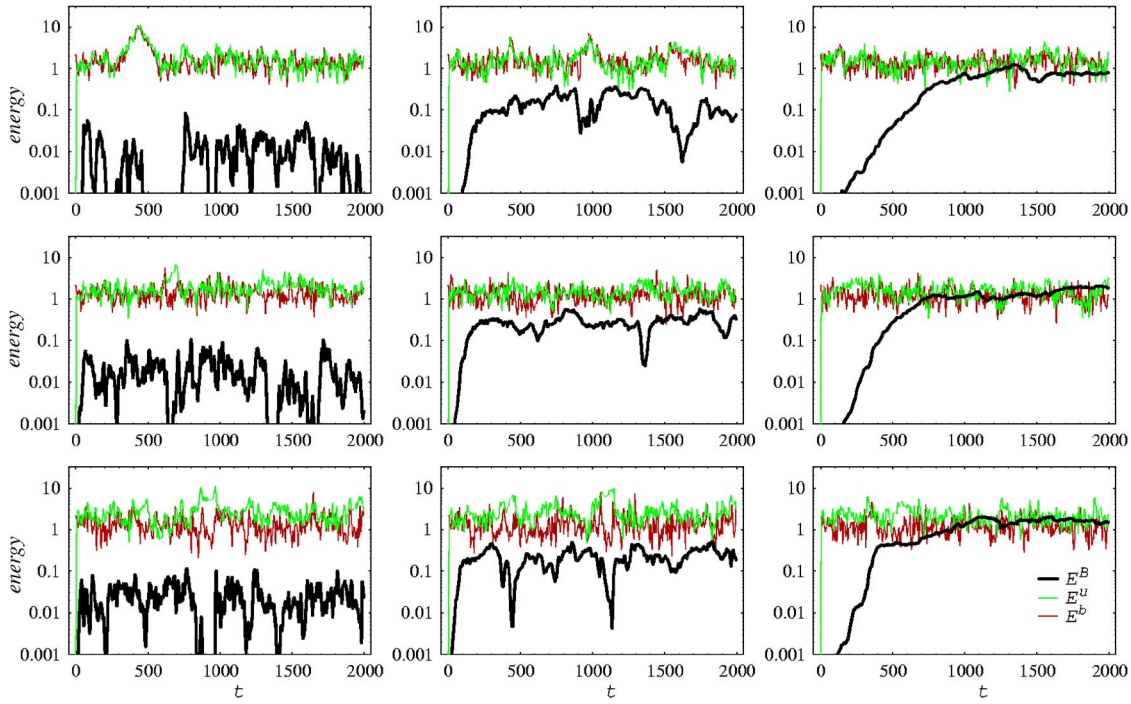

FIG. 5. (Color online) Time series for the mean magnetic field energy, small-scale magnetic energy, and kinetic energy for the same parameters as in Fig. 3 but under the constraint that *only* the magnetic field contributes to the α effect ($\alpha^u=0$). The notation is the same as in Fig. 3.

In general, we can draw the conclusion that there ar e no drastic differences between Figs. 3, 5, and 6. The growth of the magnetic field at the earlier stage (when the energy of the large-scale field remains much smaller than the turbulent energy) is essentially faster in the case with both contributions to α. A similar observation was made in [45] for the $\alpha\omega$-dynamo. In contrast, at saturated states the mean value of the large-scale magnetic field is visibly weaker. In any case, nothing like catastrophic α quenching occurs.

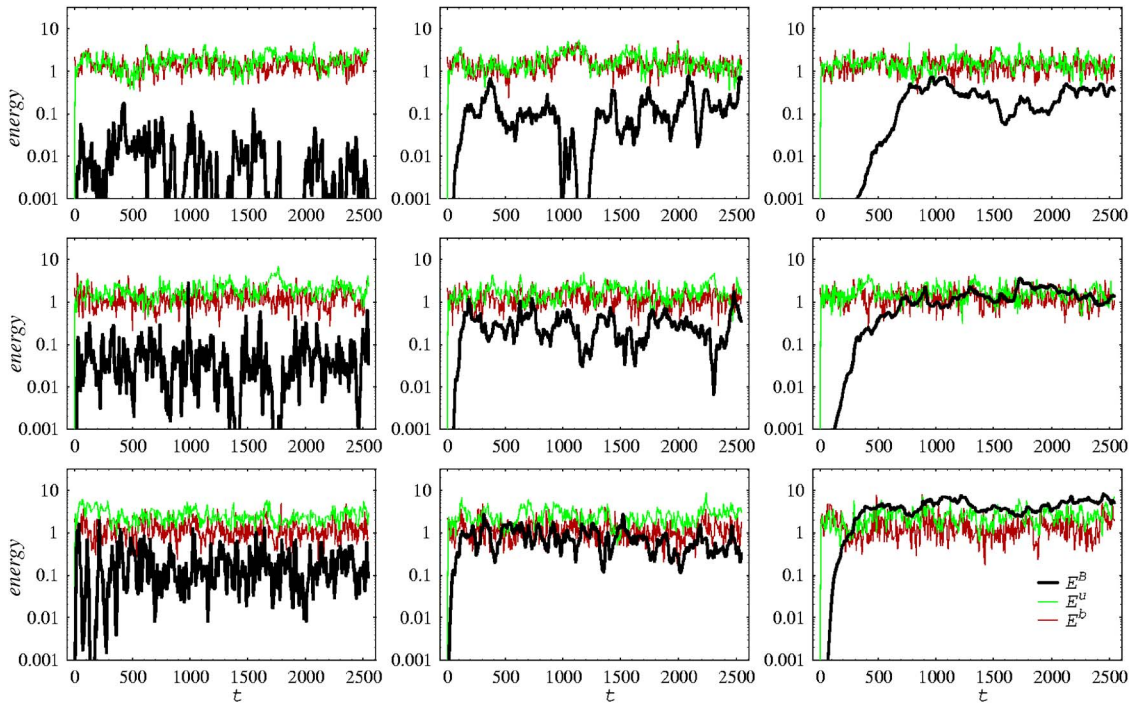

FIG. 6. (Color online) Time series for the mean magnetic field energy, small-scale magnetic energy, and kinetic energy for the same parameters as in Fig. 3, but in the case with *both* contributions to the α effect ($\alpha=\alpha^u+\alpha^b$). Notation is the same as in Fig. 3.

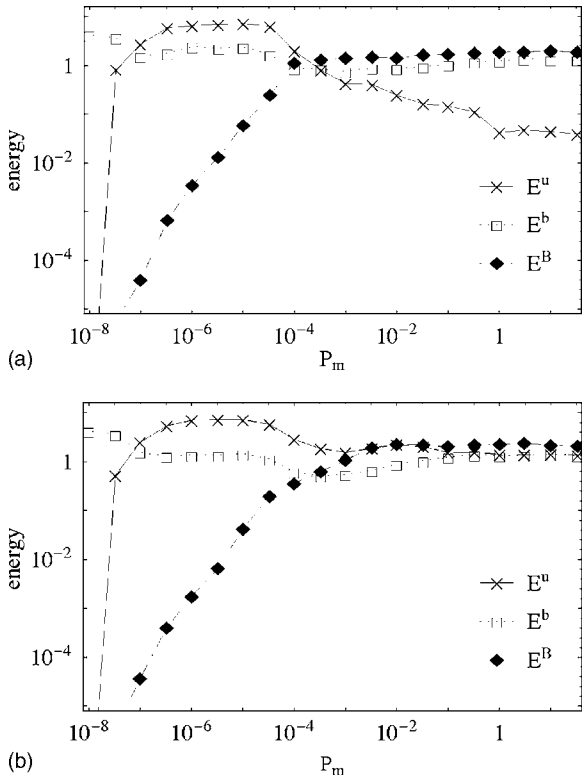

FIG. 7. Mean values of turbulent kinetic energy (empty boxes), turbulent magnetic energy (filled diamonds), and large-scale magnetic energy (crosses) versus magnetic Prandtl number. $\mathrm{Re}=10^6$, $C=0.08$, and $k_L=1/16$. (a) The case with *both* contributions to the α effect ($\alpha=\alpha^u+\alpha^b$); (b) magnetic field does not contribute ($\alpha=\alpha^u$).

C. α^2-dynamo at low magnetic Prandtl numbers

The above discussion refers to the case where $P_m \approx 1$. For cosmic turbulence, P_m differs substantially from 1. When designing the laboratory dynamo experiments, we have to restrict ourselves to very low values typical for liquid metals $P_m \approx 10^{-5}$. This is the reason why the dependence of the above results on P_m is very interesting. There is a widespread view that the case of $P_m > 1$ is basically similar to that of $P_m = 1$ while the case of $P_m < 1$ is a topic of intensive discussions [34,36,46]. The point is that the spectral range of the turbulent magnetic field is much smaller than that of the turbulent motion when $P_m \ll 1$. As a result, velocity fluctuations coexist with magnetic fluctuations within one spectral range while the other spectral range contains velocity fluctuations only. For a very low Prandtl number the magnetic spectrum can vanish and the turbulence becomes purely hydrodynamic.

We study the model with the Prandtl numbers ranging from 10^{-8} up to 10^2 and fixed parameters $\mathrm{Re}=10^6$, $C=0.08$, and $k_L=1/16$. In Fig. 7(a) energy sharing in the saturated state is plotted as a function of P_m. The mean values of the kinetic energy and the energy of small- and large-scale magnetic fields are given for various P_m. The time series and spectra for several typical values of P_m are shown in Fig. 8.

First of all, the small-scale E^b and large-scale E^B magnetic energies show a rather smooth dependence on P_m. However, the level of the kinetic energy attained depends on P_m. The small-scale dynamo does not work at $P_m < 10^{-4}$ (see the spectra in Fig. 8, right-hand bottom panel), while large-scale magnetic field is generated already at $P_m > 10^{-7}$. Note that the most efficient generation of the large-scale magnetic field happens just for $10^{-7} < P_m < 10^{-4}$, that is, the large-scale

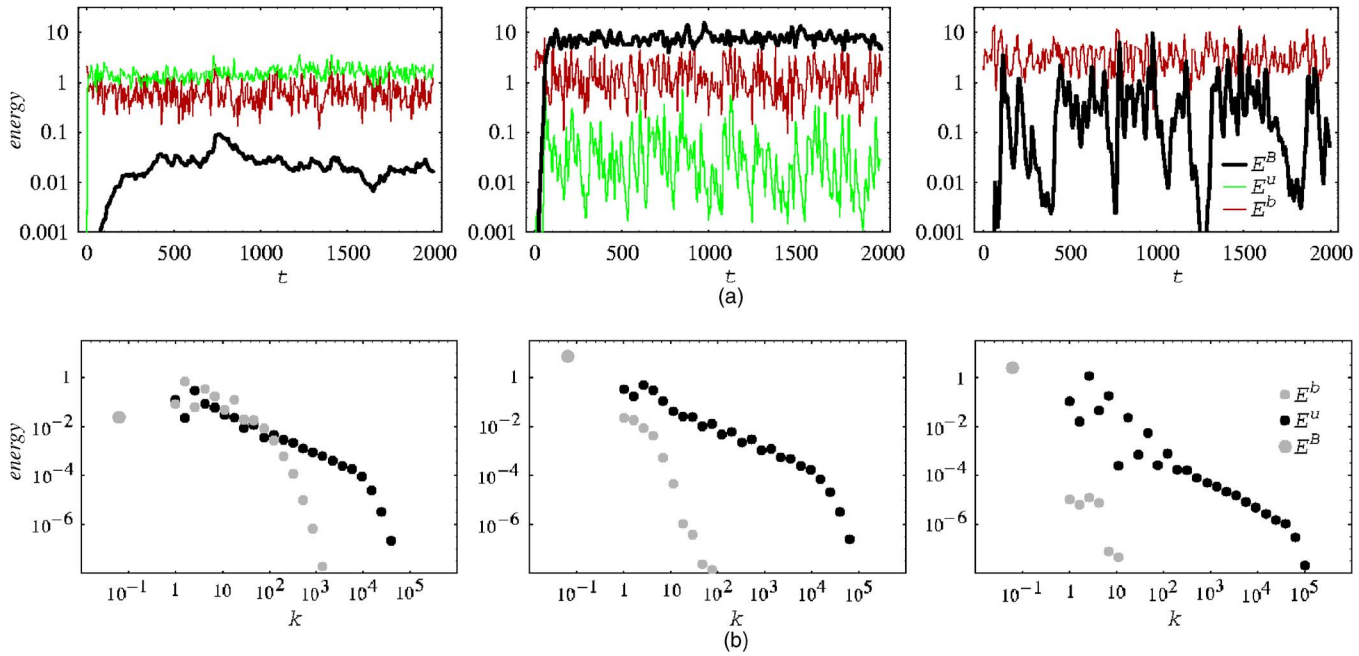

FIG. 8. (Color online) Time series (top row) for the mean magnetic field energy, small-scale magnetic energy and kinetic energy, (notation is the same as in Fig. 3) and energy spectra (bottom row) of magnetic (gray circles) and kinetic (black circles) fields for the magnetic Prandtl numbers $P_m = 3\times10^{-3}$, 10^{-5}, and 3×10^{-8} (from left to right) and $\mathrm{Re}=10^6$. The values of the large-scale magnetic field energy are shown by large gray dots.

magnetic field exceeds the equipartition level. In this range only the hydrodynamic α effect operates. Although the small-scale dynamo fails, E^b does not vanish completely in this range of P_m because the turbulent diffusion converts a part of the large-scale energy E^B into small scale. The large-scale magnetic energy generation ceases at $P_m < 10^{-7}$ because the magnetic Reynolds number becomes too small for any dynamo action. Note that the kinetic energy spectrum becomes very irregular in the large-scale range (Fig. 8, right-hand bottom panel) due to an accumulation of hydrodynamic helicity χ^u, which is provided by the force f^C and is no longer involved in the dynamo action.

A decrease of E^B occurs at $P_m > 10^{-4}$, as soon as the magnetic part of the α effect becomes comparable with the kinematic. We thus conclude that the magnetic contribution to the α effect begins to counteract the hydrodynamic contribution to the α effect provided that P_m belongs to this range of P_m. In other words, an effective α quenching occurs. To clear up once more the role of magnetic contribution into the α effect we have repeated the simulation including the action of α^u only [see Fig. 7(b)]. Here complete equipartition is observed (E_B tends to E_u for $P_m > 1$). Kinetic and magnetic small-scale fields achieve some balance and provide a constant level of α effect.

VI. SUMMARY AND DISCUSSION

We have introduced a simple model of the so-called α^2-dynamo, which combines the mean-field description of the large-scale magnetic field with the shell representation of the small-scale magnetohydrodynamic turbulence. Constructing the model we strictly fulfill the requirement of keeping all conservation laws known in MHD which efficiently restricts the variety of possible closures. The model obtained demonstrates a behavior consistent with the basic expectations of the dynamo process. In other words, the shell model technique, being a natural generalization to the Kolmogorov description of turbulence, has demonstrated its ability to provide an adequate description of mean-field dynamo action.

The model was applied to investigate such controversial issues of mean-field dynamo theory as α quenching and the role of the magnetic Prandtl number, in which an adequate description of the interactions between the large and small scales becomes crucial. The model gives no evidence for a catastrophic α quenching of dynamo action at values of the large-scale magnetic energy that approach equipartition, or low magnetic Prandtl number.

On the other hand, the model reveals some unknown features of the α^2 dynamo. In particular, we have established that the model exhibits a substantial magnetic contribution to the α effect in spite of magnetic helicity conservation and the absence of magnetic helicity separation. The importance of this possibility has long been ignored by investigators in this area. It was shown that the large-scale magnetic field generation can be based on magnetic helicity only.

One of the most important findings of our study is the dynamic nature of saturation mechanism of the dynamo action that is realized. The simultaneous cross correlation of α and the large-scale magnetic field energy E^B is negligible, while the coupling between α and E^B becomes substantial for moderate time lags.

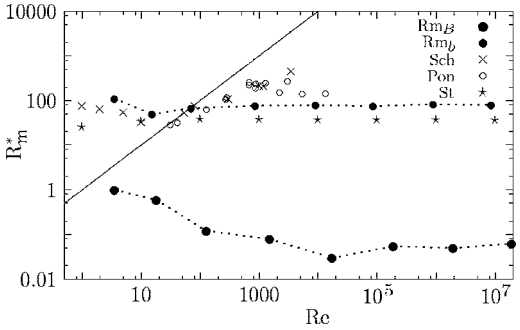

FIG. 9. Critical magnetic Reynolds number R^*_m for the large-scale α^2-dynamo (large black circles) and small-scale turbulent dynamo (small black circles) versus Reynolds number Re ($C=0.08$ and $k_L=1/16$). Results of DNS by Schekochikhin *et al.* [31] are shown by crosses; results of Ponty *et al.* [34] are shown by open circles. SM results of Stepanov and Plunian [36] are given by stars. The thin black line corresponds to $P_m=1$.

An unexpected result is the behavior of the large-scale magnetic energy with variation of P_m. Diminishing of the magnetic Prandtl number does not have an inevitable ill effect on the magnetic field generation. The most efficient large-scale dynamo operates under relatively low Prandtl numbers—then the small-scale dynamo is suppressed and a decrease of P_m can lead even to superequipartition of the large-scale magnetic field (i.e., $E_B > E_u$). In contrast, the growth of P_m does not promote the large-scale magnetic field generation. The growing counteraction of the magnetic α effect reduces the level of the mean large-scale magnetic energy at the saturated state. Note that verification of this result by direct numerical simulation is desirable.

Finally let us return to the question of how the dynamo threshold depends on the magnetic Prandtl number. Draw the neutral curves for large-scale and small-scale dynamos in the Re-R_m plane (see Fig. 9). This figure summarizes the results of numerical simulations performed for a wide range $10 < \mathrm{Re} < 10^7$ and $10^{-8} < P_m < 10^2$. Large black circles denote the critical value R^*_m obtained for the large-scale dynamo and small black circles correspond to the threshold of the small-scale (turbulent) dynamo. Note that the value of both Reynolds numbers for the neutral curve has been defined using the mean value of the kinetic energy, namely $R'_x = \sqrt{E_u} R_x$ (where R_x is Re or R_m).

Recently, the dependence of the small-scale dynamo threshold on the magnetic Prandtl number was intensively studied in DNS [30,31,33,34,46]. The results concern the range $1 \lesssim \mathrm{Re} < 13\,400$.

The authors of papers in [30,31] found an increase of the critical magnetic Reynolds number for the range $54 < \mathrm{Re} < 3500$ (corresponding points are shown in Fig. 9 by crosses), which argues for the existence of a limit $P_m \simeq \mathrm{const}$, that makes impossible the small-scale dynamo action at low magnetic Prandtl numbers. The results of the paper in [34] shown by open circles support the increase of R^*_m at moderate Reynolds numbers (from about 30 up to

about 500) but show a kind of saturation at higher Reynolds numbers ($500 < \mathrm{Re} < 3500$). This is consistent with the view that a limit $R_m^* \simeq \text{const}$ should exist at high Reynolds number (similar results are obtained in [33]—we do not show them in the figure because they would make the figure unclear). Our simulations give a straight horizontal line $R_m^* = 80 \pm 5$ for the range $100 \leqslant \mathrm{Re} \leqslant 10^7$. Note that all the DNS mentioned above studied a *pure small-scale* dynamo (without a large-scale) in *nonhelical* turbulence. In our case the velocity field is essentially helical and the threshold of small-scale dynamo action always occurs in the presence of working mean field dynamo. However, the study of small-scale MHD dynamo at low Prandtl numbers in the frame of a shell model of nonhelical turbulence [36] gives similar results (shown in Fig. 9 by stars)—R_m^* does not depend on the Reynolds number (equivalently, magnetic Prandtl number) for developed turbulence ($\mathrm{Re} > 100$).

Note that the estimates for R_m^* obtained from various models of MHD turbulence are quite similar in spite of the fact that the models are not identical. We believe that this means that the properties of a small-scale dynamo are more or less independent of the coexisting mean-field dynamo. The agreement between the estimates for R_m^* obtained in the frame of the shell models of turbulence and those from DNS support the conclusion that the shell models provide an adequate description of small-scale dynamos. Then our estimates for $\mathrm{Re} > 1000$ where DNS is impossible mean that the small-scale dynamo remains active for very low magnetic Prandtl numbers and moderate magnetic Reynolds numbers. It should be mentioned that two-point closures also give dynamo threshold independence of P_m at small P_m [47].

As for the threshold of the α^2-dynamo itself (large black circles in Fig. 9), there is a monotonous decrease of the critical magnetic Reynolds number for low and moderate Reynolds numbers (up to Re about 10^4). For fully developed turbulence ($\mathrm{Re} > 10^4$) the threshold does not depend on the Reynolds number (as well as on the magnetic Prandtl number). Let us note that the critical values of R_m obtained are unusually small (all less as unity) because the Reynolds numbers are defined by the turbulent scale. The rescaling $R_m' = 2\pi R_m / k_L \approx 10^2 R_m$ gives reasonable estimates for the critical magnetic Reynolds number for the mean-field dynamo. We conclude that the mean-field dynamo can excite the magnetic field for very moderate magnetic Reynolds numbers provided the mean hydrodynamic helicity is present.

ACKNOWLEDGMENTS

This research was supported under projects RFBR-DFG 03-02-04031, RFBR 04-02-16094, and 06-01-00234. R.S. acknowledges the support from the BRHE program. We are grateful to D. Moss for a critical reading of the manuscript.

[1] E. N. Parker, *Cosmical Magnetic Fields: Their Origin and their Activity* (Clarendon Press, Oxford, 1979).
[2] N. E. Haugen, A. Brandenburg, and W. Dobler, Phys. Rev. E **70**, 016308 (2004).
[3] W.-C. Müller and R. Grappin, Phys. Rev. Lett. **95**, 114502 (2005).
[4] A. Brandenburg and D. Sokoloff, Geophys. Astrophys. Fluid Dyn. **96**, 319 (2002).
[5] F. Krause and K.-H. Rädler, *Mean-Field Magnetohydrodynamics and Dynamo Theory* (Pergamon, New York, 1980).
[6] A. A. Ruzmaikin, D. D. Sokoloff, and A. M. Shukurov, *Magnetic Fields of Galaxies* (Kluwer, Dordrecht, 1988).
[7] R. Beck, A. Brandenburg, D. Moss, A. Shukurov, and D. Sokoloff, Annu. Rev. Astron. Astrophys. **34**, 155 (1996).
[8] A. Brandenburg and K. Subramanian, Phys. Rep. **417**, 1 (2005).
[9] V. N. Desnianskii and E. A. Novikov, Prikl. Mat. Mekh. **38**, 507 (1974).
[10] E. Gledzer, Dokl. Akad. Nauk SSSR **209**, 1046 (1973) [Sov. Phys. Dokl. **18**, 216 (1973)].
[11] T. Bohr, M. H. Jensen, G. Paladin, and A. Vulpiani, *Dynamical Systems Approach to Turbulence* (Cambridge University Press, Cambridge, UK, 1998).
[12] P. G. Frik, Magnetohydrodynamics (N.Y.) **20**, 262 (1984).
[13] C. Gloaguen, J. Léorat, A. Pouquet, and R. Grappin, Physica D **17**, 154 (1985).
[14] P. Frick and D. Sokoloff, Phys. Rev. E **57**, 4155 (1998).
[15] L. Biferale, Annu. Rev. Fluid Mech. **35**, 441 (2003).
[16] Y. Hattori, R. Rubinstein, and A. Ishizawa, Phys. Rev. E **70**, 046311 (2004).
[17] P. Frick, M. Reshetnyak, and D. Sokoloff, Europhys. Lett. **59**, 212 (2002).
[18] D. D. Sokoloff and P. G. Frick, Astron. Rep. **47**, 511 (2003).
[19] R. Stepanov, P. Frick, and D. Sokoloff, Astron. Nachr. **327**, 481 (2006).
[20] Y. B. Zeldovich, A. A. Ruzmaikin, and D. D. Sokoloff, *Magnetic Fields in Astrophysics* (Gordon and Breach, New York, 1983).
[21] G. B. Field and E. G. Blackman, Astrophys. J. **572**, 685 (2002).
[22] A. Brandenburg and C. Sandin, Astron. Astrophys. **427**, 13 (2004).
[23] N. Kleeorin, D. Moss, I. Rogachevskii, and D. Sokoloff, Astron. Astrophys. **361**, L5 (2000).
[24] N. Kleeorin, D. Moss, I. Rogachevskii, and D. Sokoloff, Astron. Astrophys. **400**, 9 (2003).
[25] I. Rogachevskii and N. Kleeorin, Phys. Rev. E **68**, 036301 (2003).
[26] A. Pouquet, U. Frisch, and J. Leorat, J. Fluid Mech. **77**, 321 (1976).
[27] A. Brandenburg and W. H. Matthaeus, Phys. Rev. E **69**, 056407 (2004).
[28] K. Subramanian and A. Brandenburg, Phys. Rev. Lett. **93**, 205001 (2004).
[29] A. Brandenburg, E. G. Blackman, and G. R. Sarson, Adv. Space Res. **32**, 1835 (2003).

[30] A. A. Schekochihin, S. C. Cowley, J. L. Maron, and J. C. McWilliams, Phys. Rev. Lett. **92**, 054502 (2004).
[31] A. A. Schekochihin, N. E. L. Haugen, A. Brandenburg, S. C. Cowley, J. L. Maron, and J. C. McWilliams, Astrophys. J. Lett. **625**, L115 (2005).
[32] S. Boldyrev and F. Cattaneo, Phys. Rev. Lett. **92**, 144501 (2004).
[33] P. D. Mininni and D. C. Montgomery, Phys. Rev. E **72**, 056320 (2005).
[34] Y. Ponty, P. D. Mininni, D. C. Montgomery, J.-F. Pinton, H. Politano, and A. Pouquet, Phys. Rev. Lett. **94**, 164502 (2005).
[35] A. P. Kazantsev, Sov. Phys. JETP **26**, 1031 (1968).
[36] R. Stepanov and F. Plunian, J. Turbul. **7**, 39 (2006).
[37] D. Sokolov, A. Shukurov, and A. Ruzmaikin, Geophys. Astrophys. Fluid Dyn. **25**, 293 (1983).
[38] U. Frisch, Z. S. She, and P. L. Sulem, Physica D **28**, 382 (1987).
[39] P. Frick, B. Dubrulle, and A. Babiano, Phys. Rev. E **51**, 5582 (1995).
[40] P. Frick, G. Boffetta, P. Giuliani, S. Lozhkin, and D. Sokoloff, Europhys. Lett. **52**, 539 (2000).
[41] T. Y. Antonov, P. G. Frick, and D. D. Sokoloff, Dokl. Akad. Nauk **63**, 271 (2001).
[42] A. S. Gabov and D. D. Sokoloff, Astron. Rep. **48**, 949 (2004).
[43] S. I. Vainshtein, Sov. Phys. JETP **67**, 517 (1975).
[44] S. I. Vainshtein, I. B. Zeldovich, and A. A. Ruzmaikin, *Turbulent Dynamo in Astrophysics* (Nauka, Moscow 1980).
[45] A. Brandenburg, S. H. Saar, and C. R. Turpin, Astrophys. J. Lett. **498**, L51 (1998).
[46] A. A. Schekochihin, S. C. Cowley, S. F. Taylor, J. L. Maron, and J. C. McWilliams, Astrophys. J. **612**, 276 (2004).
[47] J. Leorat, A. Pouquet, and U. Frisch, J. Fluid Mech. **104**, 419 (1981).